# $4f$ photoionization and subsequent Auger decay in atomic Pb: Relativistic effects

M. Patanen,[1,*] S. Urpelainen,[2] T. Kantia,[1] S. Heinäsmäki,[1] S. Aksela,[1] and H. Aksela[1]

[1]*Department of Physics, University of Oulu, P.O. Box 3000, FIN-90014 University of Oulu, Finland*

[2]*Max-lab, Lund University, Box 118, SE-22100 Lund, Sweden*

(Received 9 March 2011; published 6 May 2011)

High-resolution $4f$ photoelectron and subsequent Auger-electron spectra have been measured from free Pb atoms using synchrotron radiation. The fine structure of the spectra has been investigated theoretically by calculating the energies and intensities for $4f$ photoionization and Auger decay processes using the multiconfigurational Dirac-Fock approach. The role of the relativistic effects in the ground and singly and doubly ionized states has been studied on the basis of computed results and their comparison with experiment.

DOI: 10.1103/PhysRevA.83.053408 PACS number(s): 32.80.Fb, 32.80.Hd

## I. INTRODUCTION

Development of synchrotron radiation sources during the last twenty years with very-large-range tunable photon energies and high intensities has lead to a revolution in the field of electron spectroscopy. Due to the very high inherent photon flux from synchrotron radiation sources, very narrow photon energy bands can be selected by high-resolution monochromators to ionize atoms in the target volume. The usable photon bandwidths in gas phase measurements can typically be some tens of meV in the soft-x-ray region and even in the $\mu$eV range for uv radiation. High resolution has enabled determination of lifetimes of atomic states much more accurately than before.

Most of the elements are solids in their natural form but evaporate usually as free atoms or small molecules when heated in vacuum. Only rare gases appear as free atoms in their natural form. Therefore vapor phase studies are a very important source of experimental information about free atoms in order to extend the knowledge of atomic effects beyond what is seen in rare gases only. The basic difficulty in vapor studies is the low target density in the vapor beams, which correspond typically to partial pressures of $10^{-6}$–$10^{-5}$ mbar in the target volume. Combining the development of ovens for vapor production with the high photon flux at today's synchrotron sources, numerous studies of free atoms have been carried out by our group during the last few years (see e.g., [1–5] and references therein). Traditionally, resistively or inductively heated ovens have been used for metal vapor production [6–13]. Recently, for example, $3d$ transition metals have been intensively studied by producing the atomic beam with ovens (see e.g., [14] and references therein) and, besides using direct heating to high temperatures, free neutral atoms have also been produced by magnetron-based sources [15].

In this paper we present results of our recent experiments on $4f$ photoionization and Auger decay in atomic lead. Pb is an interesting sample for investigations as it is highly toxic but yet it and its compounds are commonly used in several applications. Pb is used in the electronic industry, to stabilize certain plastics, in lead-acid batteries, or in leaded fuel, to name a few applications. Furthermore, relativistic effects created by strong spin-orbit interactions, which are typical for heavy atoms, were found to play a prominent role in ground and valence-ionized states of atomic Pb [4,16] as well as in valence shells of lead compounds [17]. The news that cars start due to relativity in the lead-acid battery [17] attained notable attention very recently [18].

Ionization of a deeper $4f$ subshell of atomic Pb, studied in this work and introduced also in Ref. [19], is assumed to display even stronger relativistic effects. This assumption is shown to be correct in the present work. When the core-hole state rapidly decays via Auger-electron emission, producing two holes in the $5d$ subshell, reorganization of the outermost orbitals may take place. In this paper we will demonstrate that such two-hole states no longer fully retain their relativistic character, but the states are better described by an intermediate-coupling scheme, where not only the spin-orbit interaction but also the electrostatic interaction plays a role. Photoelectron and subsequent Auger-electron spectra taken at a modern synchrotron radiation source have allowed us to image the characters of the deep $4f$ core-hole and the double $5d$ hole states, and the behavior of the outer valence $6p^2$ configuration in the presence of deeper holes. The relativistic Dirac-Fock method is used to characterize the nature of atomic states.

## II. EXPERIMENTAL

The experiments were carried out using synchrotron radiation from undulator beamline I411 [20] at the MAX II storage ring at the MAX-laboratory in Lund, Sweden. The beamline is equipped with a high-resolution SX-700 plane grating monochromator [21]. An inductively heated oven was used to evaporate the solid Pb sample. This heating method has turned out to be very convenient in generating high temperatures for low-volatile samples. It is much faster than resistive heating in reaching the operating temperatures, but due to the generated magnetic fields the heating usually needs to be pulsed: when the heating is applied the electron signal from the detector is rejected. This causes some unavoidable decrease in data collection efficiency, typically 10% to 30%. Our present setups have been described in more detail in [22–24]. The estimated oven temperature was 720 °C corresponding to a vapor pressure of about $10^{-3}$ mbar inside the heated volume.

A modified Scienta SES-100 electron energy analyzer [23] was used to record the emitted electrons at the "magic" 54.7° angle with respect to the polarization vector of the

*Current address: Synchrotron SOLEIL, L'Orme des Merisiers, Saint-Aubin, BP 48, F-91192 Gif-sur-Yvette Cedex, France.

 

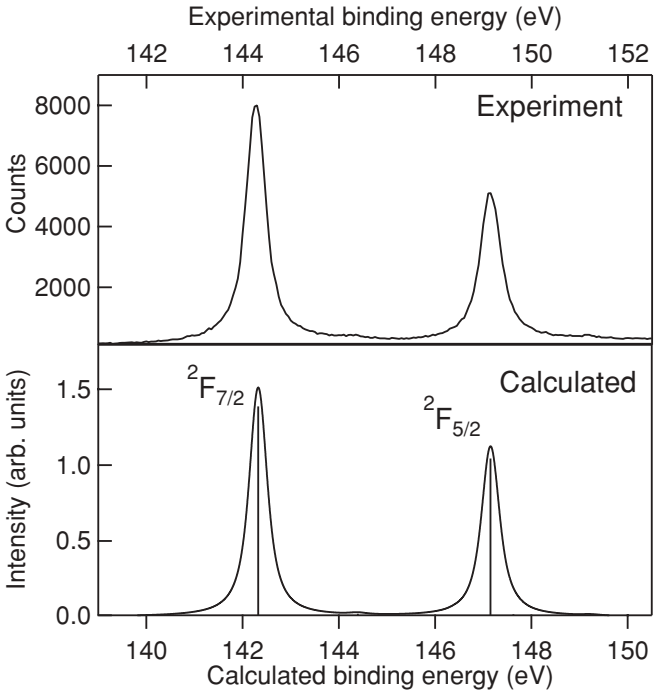


FIG. 1. Experimental ($h\nu = 200$ eV) and calculated $4f$ photoelectron spectra. Experimental data was accumulated for 215 minutes.

horizontally polarized synchrotron radiation, corresponding to the angle-independent measurements. The electron spectrometer is equipped with a resistive anode positive sensitive detection system making it possible to gate the electron detection during short inductive heating intervals in order to avoid disturbances of the high-frequency induction field. The energy of the ionizing radiation was 200 eV in the measurements of Pb vapor. The $4f$ photoelectron spectrum (PES) was calibrated by introducing Kr gas into the interaction region and recording the Kr $3d$ photoelectron spectrum simultaneously with the vapor lines. The values 93.788 eV and 95.038 eV were used for binding energies of the Kr $3d_{5/2}$ and $3d_{3/2}$ lines, respectively, from King *et al.* [25]. The kinetic energies of the Auger-electron spectrum were calibrated using the Kr $MNN$ Auger transition, as per Ref. [26].

Pb $4f$ photolines recorded using 200 eV photons are shown in Fig. 1. We obtained the binding energies of $144.30 \pm 0.03$ eV and $149.17 \pm 0.03$ eV for atomic Pb $^2F_{7/2}$ and $^2F_{5/2}$ states, respectively. Line shape analysis gave $\Gamma_{4f_{5/2}} = 290 \pm 10$ meV and $\Gamma_{4f_{7/2}} = 280 \pm 10$ meV for the total inherent Lorentzian widths. Instrumental broadening for photolines was estimated with help of Kr $3d$ photolines (full width at half maximum, FWHM = 88 meV from [27]), and it was found to be a Voigt shape with FWHM = 280 meV. The broadening caused by the photon beam seems to have a Lorentzian shape with FWHM = 120 meV. Using the Kr $M_{4,5}N_{2,3}N_{2,3}$ Auger lines for calibration, the instrumental broadening for Auger lines caused by the electron energy analyzer was estimated to be a Gaussian shape with FWHM = 220 meV.

The $4f$ Auger-electron spectrum to the $5d^{-2}$ final states of atomic Pb is displayed in Fig. 2. The kinetic energy of the strongest peak, labeled A in Fig. 2, was determined to be $80.33 \pm 0.1$ eV. No attempt to fit all the features in the Auger

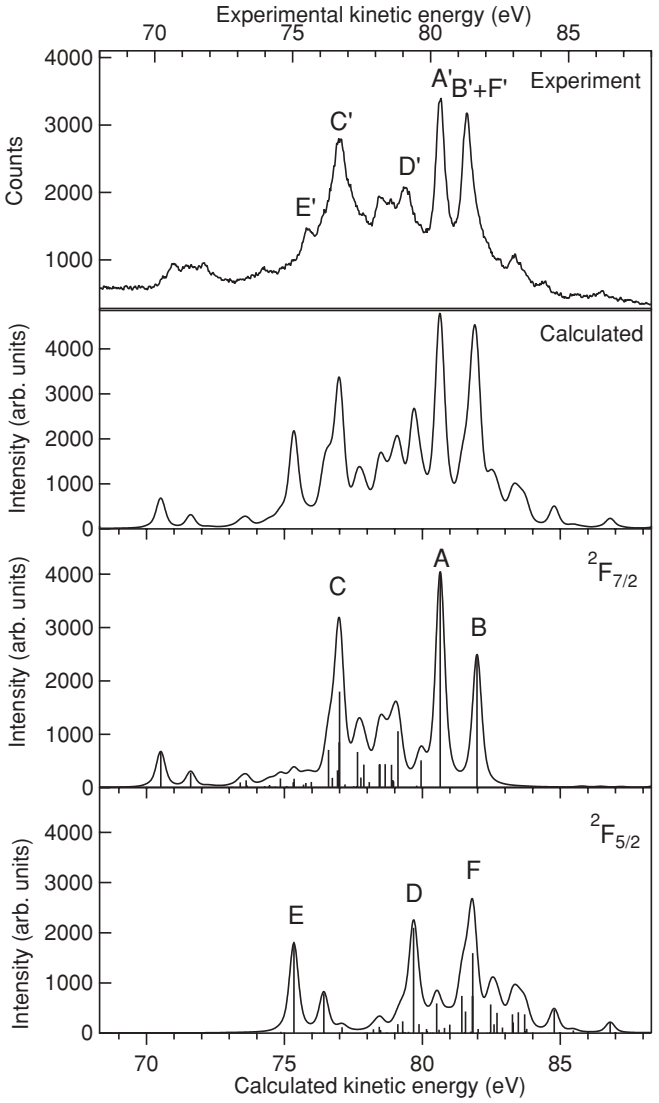


FIG. 2. Experimental $N_{6,7}O_{4,5}O_{4,5}$ Auger-electron spectrum measured with a photon energy of 200 eV and theoretical Auger transitions from the $^2F_{7/2}$ and $^2F_{5/2}$ initial states. Labels A–F refer to Table I. Experimental data were accumulated for 400 minutes.

spectrum was made due to numerous overlapping peaks. Visual comparison with the calculated spectrum with identification of strongest peaks, however, allowed us to understand the characters of the states involved in the Auger decay, as will be shown below.

## III. DISCUSSION

In order to investigate the electronic structure and the transition energies from the ground state to the single $4f$ core hole and further to the double $5d^{-2}$ states of Pb, *ab initio* calculations based on the relativistic Dirac-Fock method were performed. The energies were calculated as extended average level calculations. The calculated binding energies [$E_b(4f_{7/2}) = 143.92$ eV and $E_b(4f_{5/2}) = 148.72$ eV] were found to deviate less than 0.7 eV from the experimental values. The kinetic energy of peak A in the Auger spectrum (Fig. 2)

was found to agree well with the calculated value of 80.65 eV, with the discrepancy being only 0.3 eV.

In heavy atoms, relativistic effects are strong, and in the calculations the atomic states are taken to be the eigenstates of total angular momentum $J$ and the parity $\Pi$. Wave functions for the atomic orbitals were calculated using the GRASP92 code [28], and the mixing coefficients for the states as well as energies were obtained with the GRASP2K package [29]. Transformation to the $LS$ coupling was performed using the utilities of the RATIP package [30].

Relative photoionization probabilities were estimated using an approximative scheme where the frozen-core photoionization amplitudes were computed by keeping the single-particle ionization rates constant for each state, which (neglecting the energy-dependent prefactors) leads to the intensity formula

$$Q_f(J_f) = \frac{2J_f+1}{2J_0+1}\left|\sum_{rs} c_{fr}c_{0s}\right|^2 \delta_{\alpha_f\alpha_0}. \quad (1)$$

Here the symbol $\delta_{\alpha_f\alpha_0}$ signifies the frozen-core approximation, meaning that each final ionic state mixing coefficient $c_{fr}$ is multiplied with the coefficient $c_{0s}$ of the corresponding "parent" configuration-state function (CSF) of the initial state. The parent is defined as that CSF which gives rise to the final ionic state CSF after removing one electron, so that the configuration of the other electrons remains intact. Equation (1) is valid for an arbitrary open-shell atom, provided that the shell from which the electron is removed is initially closed and that the electrons of that shell are coupled after all the other electrons to form the total CSF [31].

The Auger-electron emission probability within the two-step formulation can be written as

$$n_A(J) = \frac{Q_f R_{fJ}}{P_f}, \quad (2)$$

where $R_{fJ}$ is the Auger rate from the ionic one-hole state to the final two-hole state denoted by its angular momentum $J$ and $P_f = \sum_J R_{fJ}$ is the total (nonradiative) decay probability of the one-hole state. Partial Auger decay rates from the 4$f$ ionized states were obtained using unpublished routines of the RATIP package [30]. Lifetimes of the 4$f$ hole states were determined by taking the inverse of the sum of the partial transition rates to all possible Auger final states. Photoelectron and Auger-electron spectra for comparison with the experimental ones were generated using the calculated energies, transition rates, and lifetimes, and the spectra were convoluted by the instrumental function corresponding to the experimental broadening.

There is only one state populated in the ground state of Pb, which is described using nonrelativistic electronic configuration andthe $LSJ$ spectral term as [Xe]$4f^{14}5d^{10}6s^26p^2$ ($^3P_0$). The nonrelativistic configuration $6p^2$ distributes to three relativistic configurations: $6p^2_{1/2}$, $6p^1_{1/2}6p^1_{3/2}$, and $6p^2_{3/2}$. Spin-orbit coupling is so strong that the $6p_{1/2}$ and $6p_{3/2}$ orbitals are well separated and, in the ground state of Pb, the outermost subshell is formed from the closed $6p_{1/2}$ relativistic configuration. According to calculations, the energy difference with the next level was (experimental values in parentheses) 0.85 eV (0.97 eV [32]). In the final state of 4$f$ ionization the outermost subshell retains its relativistic character $6p^2_{1/2}$, which does not couple to the ionized 4$f$ orbital, and the strongest peaks seen in the PES are the $^2F_{7/2}$ and $^2F_{5/2}$ states. Purity of the $^2F_{7/2}$ and $^2F_{5/2}$ states according to the calculations is 93%.

Calculations of the total decay rate give widths to both 4$f$ ionized states that are too small (223 meV and 228 meV for the $^2F_{7/2}$ and $^2F_{5/2}$ states, respectively). The calculated Auger decay is strongest (>70% of the total rate) to the $5d^{-2}$ final states in the kinetic energy region of 70 to 90 eV, but the partial decay rate to the low kinetic energy part (below 10 eV of kinetic energy) of the spectrum is also significant. These low kinetic energy transitions are typically not well predicted by calculations because of the uncertainties in the construction of the continuum wave functions and the limited configuration-interaction (CI) space adopted in the computations. This is most probably the reason for the underestimation of the natural widths of the lines. As the detection of the low kinetic energy electrons is very difficult with our spectrometer, closer investigation of this assumption was not possible. Good agreement between the calculated and experimental photoelectron spectra is seen from Fig. 1.

Figure 2 displays the Auger-electron spectrum, which is created from the decay of the 4$f$ core-hole $^2F_{7/2}$ and $^2F_{5/2}$ states to the $5d^{-2}$ final state configuration. The uppermost spectrum is experimental, the next is the calculated spectrum, and the two spectra below show the separate contributions from the decay of the $^2F_{7/2}$ and $^2F_{5/2}$ states, respectively. By assuming that the two-hole final state fully retains its relativistic character, one would expect that 9 multiplets (in analogy to the $LSJ$ coupled terms $^1S_0$, $^1D_2$, $^1G_4$, $^3P_0$, $^3P_1$, $^3P_2$, $^3F_2$, $^3F_3$, and $^3F_4$) get populated in Auger decay. This is because the $6p_{1/2}$ orbital would remain occupied by two electrons forming a closed shell, and the $6p_{3/2}$ orbital would remain empty. A similar peak structure as seen in the $4f^{-1} \rightarrow 5d^{-2}$ Auger spectrum of mercury (ground-state configuration [Xe]$4f^{14}5d^{10}6s^2$) [33] would be expected. However, the Auger spectrum of Pb shows features which are typical for a spectrum taken from an open-shell atom. This is seen especially in the calculated stick spectra, which display a multitude of peaks which then form the broad structures in the sum spectrum. Calculations reproduce the experiment well enough that conclusions about the character of the states can be drawn. Next we will concentrate on the strongest lines in the spectrum and follow their assignment from the calculations.

Table I lists the six strongest lines in the Auger spectrum labeled in Fig. 2 by A to F and gives their kinetic energies and assignments of final states both in $jj$ and in $LSJ$ coupling. Energy splitting of the final states is somewhat overestimated by calculations, which is a typical feature if mixture with higher excitations is excluded [1]. As seen from the weights of the $LS$ states, the $LS$ coupling scheme fails completely in describing the states. We will still use the leading $LS$ terms of the $5d^{-2}$ configuration only in order to use a simple assignment for the lines and to see the analogy to a closed-shell system. Large deviations from the pure $LSJ$ coupling is easy to understand as the spin-orbit splitting of the 5$d$ orbital is large and thus the parent states are already strongly mixed, as was also seen in the $4f^{-1} \rightarrow 5d^{-2}$ Auger decay of Hg [33]. In the decay of the $^2F_{7/2}$ state of Pb, the most strongly populated final states are the parent states $^1D_2$ (peak A), $^3F_2$ (peak B),

TABLE I. Calculated $N_{6,7}O_{4,5}O_{4,5}$ Auger kinetic energies (eV) and two leading $jj$- and $LSJ$-coupled CSFs for the Auger final states. Numbers before CSF indicate the weight of the CSF in the atomic states function. In $LSJ$ coupling the first term in parentheses indicates how the $5d$ electrons have been coupled, and the second term indicates how the $6p$ electrons have been coupled to the parent $LS$ terms. The last term is the total term symbol of the state. Labels A–F refer to peaks in Fig. 2, and the terms $^2F_{7/2}$ and $^2F_{7/2}$ show the Auger initial state (final state of photoionization) in Fig. 1.

| Label Fig. 2 | Initial State | Kinetic Energy (eV) | Final States | | | |
|---|---|---|---|---|---|---|
| | | | $jj$ Coupling | | $LSJ$ Coupling | |
| A | $^2F_{7/2}$ | 80.65 | $0.855d^4_{3/2}5d^4_{5/2}6p^2_{1/2}$ | $0.055d^4_{3/2}5d^4_{5/2}6p^1_{1/2}6p^1_{3/2}$ | $0.15\ (^1D^3P)^3F_2$ | $0.10(^1D^3P)^3D_2$ |
| B | $^2F_{7/2}$ | 81.98 | $0.875d^4_{3/2}5d^4_{5/2}6p^2_{1/2}$ | $0.055d^3_{3/2}5d^5_{5/2}6p^2_{1/2}$ | $0.23\ (^3F^3P)^5F_4$ | $0.22(^3F^3P)^5D_4$ |
| C | $^2F_{7/2}$ | 77.00 | $0.585d^3_{3/2}5d^5_{5/2}6p^2_{1/2}$ | $0.155d^3_{3/2}5d^5_{5/2}6p^1_{1/2}6p^1_{3/2}$ | $0.32(^1G^3P)^3G_4$ | $0.12\ (^1G^3P)^3H_4$ |
| D | $^2F_{5/2}$ | 79.68 | $0.445d^2_{3/2}5d^6_{5/2}6p^2_{1/2}$ | $0.135d^4_{3/2}5d^4_{5/2}6p^2_{3/2}$ | $0.16\ (^1D^3P)^3F_2$ | $0.13\ (^3P^1D)^3D_2$ |
| E | $^2F_{5/2}$ | 75.34 | $0.515d^4_{3/2}5d^4_{5/2}6p^2_{1/2}$ | $0.155d^3_{3/2}5d^5_{5/2}6p^2_{3/2}$ | $0.37\ (^1S^3P)^3P_0$ | $0.17\ (^1S^3P)^5D_0$ |
| F | $^2F_{5/2}$ | 81.82 | $0.585d^3_{3/2}5d^5_{5/2}6p^2_{1/2}$ | $0.155d^3_{3/2}5d^5_{5/2}6p^1_{1/2}6p^1_{3/2}$ | $0.32\ (^1G^3P)^3G_4$ | $0.12\ (^1G^3P)^3H_4$ |

and $^1G_4$ (peak C). The $^2F_{5/2}$ hole states decay strongly to $^1D_2$ (peak D) and to $^1G_4$ (peak F) parent states as well, but also to $^1S_0$ (peak E). There is some resemblance with the spectrum of Hg [33]: the same parents were the strongest lines in the decay of the $^2F_{5/2}$ hole state and the $^3F_2$ and $^1G_4$ states were also strongly populated in the decay of the $^2F_{7/2}$ hole state. In the Auger decay of Pb compared to Hg, however, many more final states get populated. Using the language of configuration interaction, we may interpretate that CI in the final state of the Auger decay redistributes the intensity between the states according to the mixing of relativistic configurations $6p^2_{1/2}$, $6p^1_{1/2}6p^1_{3/2}$, and $6p^2_{3/2}$. This is actually seen if we take a look at the $jj$-coupled functions in Table I. The $6p^2_{1/2}$ closed shell character is not complete—there is a clear mixing with relativistic configurations $6p^1_{1/2}6p^1_{3/2}$ and $6p^2_{3/2}$. The mixing turns out to be stronger for states populated from the decay of the $^3F_2$ state.

The removal of the electrons from the $5d$ shells affects the role played by spin-orbit and electrostatic effects. A closed shell has no electrostatic effect on outside electrons, but in the two-hole state the electrostatic force quickly becomes comparable to the spin-orbit interaction (judged from the splitting of some "main" contributing component lines in the spectrum), and in this sense the relativistic effects may be diminished by electrostatic ones even in heavy elements like Pb. Quantitatively, the interplay between the relativistic and electrostatic effects can be estimated from the strength of the Coulomb matrix elements in the open shells compared to the observed spin-orbit splitting. The contributions due to Coulomb interactions are visible as mixing of configurations and the magnitude depends on the "direct" Coulomb integrals $F^k(a,b)$ for $k > 0$ and on the exchange integrals $G^k(a,b)$, measuring the deviation of the energy from the average-of-configuration energy. In our case there are two comparisons to be made: the amount of electrostatic interaction between the $6p_{1/2}$ and $6p_{3/2}$ orbitals in the Auger initial state, as compared to the splitting of the $4f$ lines, and the Coulomb interactions among the $6p$ and $5d$ orbitals in the Auger final state. In the first case the dominant effect is indeed spin-orbit splitting, since the possible contributing electrostatic contributions $G^2(6p_{1/2},6p_{3/2})$ and $F^2(6p_{3/2},6p_{3/2})$ are both of the order of 2 eV (apart from small contributions coming from angular momentum coupling factors), which is smaller than the observed spin-orbit splitting. In the final state, on the other hand, the $5d$ shell has the main contributing matrix elements $F^2(5d_{3/2},5d_{3/2})$, $F^2(5d_{3/2},5d_{5/2})$, and $F^2(5d_{5/2},5d_{5/2})$, which have magnitudes 10 to 14 eV, again apart from coupling factors. These matrix elements are thus capable of providing the necessary electrostatic contributions for causing mixing of the states in the Auger spectrum, overcoming the relativistic (spin-orbit) effects.

## IV. CONCLUSIONS

The single $4f$ core-hole states were found to display a very clear relativistic character. This holds for both the $4f$ core holes and the outermost valence. The double $5d^{-2}$ hole states of Pb, however, show a strong mixture both of the relativistic parent holes on the $5d$ orbital, as of the outermost relativistic configurations $6p^2_{1/2}$, $6p^1_{1/2}6p^1_{3/2}$, and $6p^2_{3/2}$. Coulomb interactions between the two $5d$ holes compete with the spin-orbit interaction and the states no longer retain their clear and complete relativistic character. However, they are closer to $jj$ coupling than to $LS$ coupling. Electrostatic interactions in the $5d$ two-hole state, which creates a large splitting of the $LS$ parent states, plays an important role and disturbs the clear closed-shell character with the $6p^2_{1/2}$ configuration on the outermost shell. This effect becomes clear in Auger decay, which shows features typical for an open-shell atom. Comparison between experiment and calculations allowed us to image the characters of the states. Similar effects may become visible in multiply ionized states of heavy atoms which become accessible when radiated at free electron lasers.

## ACKNOWLEDGMENTS

This work was financially supported by the Research Council for Natural Sciences of the Academy of Finland and the European Community Research Infrastructure Action under the FP6 "Structuring the European Research Area" Program (through the Integrated Infrastructure Initiative "Integrating Activity on Synchrotron and Free Electron Laser Science"). MP would like to thank the Magnus Ehrnrooth foundation for

financial support. SU would like to acknowledge the Research Council for Natural Sciences and Engineering of the Academy of Finland (Grant No. 135871) and Lund's University for financial support. We are grateful to S. Fritzsche for allowing access to unpublished routines in the RATIP [30] package. We thank Pentti Kovala for his assistance during the mechanical design of the experimental apparatus. We thank also the staff of MAX-laboratory for their assistance during the experiments.

[1] M. Patanen, S. Heinäsmäki, S. Urpelainen, S. Aksela, and H. Aksela, Phys. Rev. A **81**, 053419 (2010).
[2] M. Huttula, L. Partanen, A. Mäkinen, T. Kantia, H. Aksela, and S. Aksela, Phys. Rev. A **79**, 023412 (2009).
[3] T. Kantia, S. Aksela, P. Turunen, L. Partanen, and H. Aksela, J. Phys. B **43**, 205002 (2010).
[4] S. Urpelainen, S. Heinäsmäki, M.-H. Mikkelä, M. Huttula, S. Osmekhin, H. Aksela, and S. Aksela, Phys. Rev. A **80**, 012502 (2009).
[5] A. Sankari, R. Sankari, S. Heinäsmäki, M. Huttula, S. Aksela, and H. Aksela, Phys. Rev. A **77**, 052703 (2008).
[6] Y. S. Khodeyev, H. Siegbahn, K. Hamrin, and K. Siegbahn, Chem. Phys. Lett. **19**, 16 (1973).
[7] W. Mehlhorn, B. Breuckmann, and D. Hausamann, Phys. Scr. **16**, 177 (1977).
[8] R. Bruhn, B. Sonntag, and H. W. Wolff, J. Phys. B **12**, 203 (1979).
[9] J. M. Dyke, N. K. Fayad, A. Morris, and I. R. Trickle, J. Phys. B **12**, 2985 (1979).
[10] R. Bruhn, E. Schmidt, H. Schröder, and B. Sonntag, J. Phys. B **15**, 2807 (1982).
[11] G. Materlik, B. Sonntag, and M. Tausch, Phys. Rev. Lett. **51**, 1300 (1983).
[12] H. Derenbach, H. Kossmann, R. Malutzki, and V. Schmidt, J. Phys. B **17**, 2781 (1984).
[13] E. Schmidt, H. Schröder, B. Sonntag, H. Voss, and H. E. Wetzel, J. Phys. B **18**, 79 (1985).
[14] M. Martins, K. Godehusen, T. Richter, P. Wernet, and P. Zimmermann, J. Phys. B **39**, R79 (2006).
[15] M. Tchaplyguine *et al.*, Rev. Sci. Instrum. **77**, 033106 (2006).
[16] N. Sandner, V. Schmidt, W. Mehlhorn, F. Wuilleumeir, M. Y. Adam, and J. P. Desclaux, J. Phys. B **13**, 2937 (1980).
[17] R. Ahuja, A. Blomqvist, P. Larsson, P. Pyykkö, and P. Zaleski-Ejgierd, Phys. Rev. Lett. **106**, 018301 (2011).
[18] Reviews of article [17] have been published in popular magazines like *The Economist (Einstein and car batteries: A spark of genius)* Jan. 13, 2011 and *New Scientist (Car batteries run on relativity)*, Jan. 14, 2011.
[19] M. Patanen, S. Aksela, S. Urpelainen, T. Kantia, S. Heinäsmäki, and H. Aksela, J. Electron Spectrosc. Relat. Phenom. **183**, 59 (2011).
[20] M. Bässler *et al.*, Nucl. Instrum. Methods Phys. Res., Sect. A **469**, 382 (2001).
[21] S. Aksela, A. Kivimäki, R. Nyholm, and S. Svensson, Rev. Sci. Instrum. **63**, 1252 (1992).
[22] M. Huttula, K. Jänkälä, A. Mäkinen, H. Aksela, and S. Aksela, New J. Phys. **10**, 013009 (2008).
[23] M. Huttula, S. Heinäsmäki, H. Aksela, and E. Kukk, J. Electron Spectrosc. Relat. Phenom. **156**, 270 (2007).
[24] M. Huttula, L. Partanen, A. Mäkinen, T. Kantia, H. Aksela, and S. Aksela, Phys. Rev. A **79**, 023412 (2009).
[25] G. C. King, M. Tronc, F. H. Read, and R. C. Bradford, J. Phys. B **10**, 2479 (1977).
[26] H. Aksela, S. Aksela, and H. Pulkkinen, Phys. Rev. A **30**, 2456 (1984).
[27] M. Jurvansuu, A. Kivimäki, and S. Aksela, Phys. Rev. A **64**, 012502 (2001).
[28] F. A. Parpia, C. F. Fischer, and I. P. Grant, Comput. Phys. Commun. **94**, 249 (1995).
[29] P. Jönsson, X. He, C. F. Fischer, and I. P. Grant, Comput. Phys. Commun. **177**, 597 (2007).
[30] S. Fritzsche, J. Electron Spectrosc. Relat. Phenom. **114–116**, 1155 (2001).
[31] M. Huttula, E. Kukk, S. Heinäsmäki, M. Jurvansuu, S. Fritzsche, H. Aksela, and S. Aksela, Phys. Rev. A **69**, 012702 (2004).
[32] D. Wood and K. L. Andrew, J. Opt. Soc. Am. **58**, 818 (1968).
[33] H. Aksela, S. Aksela, J. S. Jen, and T. D. Thomas, Phys. Rev. A **15**, 985 (1977).